Title

Fos-CreER-based genetic mapping of forebrain regions activated by acupuncture.

Journal

The Journal of Comparative Neurology, 528(6)

Authors

Guo, Zhiling
Lin, Xiaoxiao
Samaniego, Tracy
et al.

Publication Date

2020-04-01

DOI

10.1002/cne.24789

Peer reviewed

HHS Public Access

Author manuscript

J Comp Neurol. Author manuscript; available in PMC 2021 April 01.

Published in final edited form as:

J Comp Neurol. 2020 April ; 528(6): 953–971. doi:10.1002/cne.24789.

Fos-CreER Based Genetic Mapping of Forebrain Regions Activated by Acupuncture

Zhiling Guo[1], **Xiaoxiao Lin**[2], **Tracy Samaniego**[1], **Alexander Isreb**[2], **Stacey Cao**[2], **Shaista Malik**[1], **Todd C. Holmes**[3], **Xiangmin Xu**[2]

[1]Department of Medicine and Susan Samueli Integrative Health Institute, University of California at Irvine, Irvine, CA 92697-4075, USA

[2]Department of Anatomy and Neurobiology, University of California at Irvine, Irvine, CA 92697-1275, USA

[3]Department of Physiology and Biophysics, University of California at Irvine, Irvine, CA 92697-4850, USA

Abstract

Acupuncture increasingly is accepted as a potential therapy for many diseases in the Western world. However, the mechanism of acupuncture is not well understood mechanistically. We have established that manual acupuncture (MA) at the Neiguan (P6) acupoint inhibits excitatory cardiovascular reflex responses through modulation of the autonomic nervous system in the brainstem. It is unclear whether P6 MA activates neurons in the brain regions beyond the brainstem. Thus, we mapped P6 specific neural activation by MA in the forebrain using the Fos-CreER; Ai9 mice model, which allows for enhanced sensitivity and efficiency compared to conventional immunohistochemical staining. Compared to sham-MA control without manual stimulation, we find that MA at P6 markedly increases c-Fos positive neurons in a number of the forebrain regions (n=5 in each group). These activated regions include accumbens nucleus, caudate putamen, claustrum, bed nucleus of the stria terminalis, amygdaloid nucleus, ventral posterior division of the thalamic nucleus, paraventricular hypothalamic nucleus, arcuate hypothalamic nucleus, primary and secondary sensory cortex, ectorhinal cortex, and dorsolateral entorhinal cortex. As MA at P6 activates neurons in relatively broad brain networks beyond the brainstem, our data suggest that acupuncture at this acupoint has the potential to influence physiological functions associated with autonomic and non-autonomic nervous systems through its effects on multiple brain regions.

Address for correspondence: Zhi-Ling Guo, MD, PhD, Department of Medicine, University of California, Irvine, Irvine, CA 92697-4075, USA, zguo@uci.edu, Tel: 949-824-8161, Xiangmin Xu, PhD, Department of Anatomy & Neurobiology, University of California, Irvine, Irvine, CA 92697-1275, USA, xiangmin.xu@uci.edu, Tel: 949 824-0040.

AUTHOR CONTRIBUTIONS

Z.G. and X.X. designed the study; Z.G., X.L., A.I., and S.C. conducted experiments; Z.G., T.S., S.M. X.X. analyzed the data; Z.G., T.S., and X.X. drafted the manuscript; Z.G., T.S., S.M., T.C.H, and X.X. reviewed and edited the manuscript.

DATA AVAILABILITY STATEMENT

The data that support the findings of this study are available from the corresponding author upon reasonable request.

CONFLICT OF INTEREST

The authors declare no potential conflicts of interest.

We have established that manual acupuncture (MA) at the Neiguan (P6) acupoint modulates cardiovascular responses through influence on the autonomic nervous system in the brainstem. It is unclear about neuronal activation by P6 MA in the brain regions beyond the brainstem. In the present study, we find that in the Fos-CreER; Ai9 mice model, MA at P6 markedly increases c-Fos positive neurons in a number of forebrain regions, including somatosensory cortex (S), ectorhinal cortex (Ect), and dorsolateral entorhinal cortex (DLEnt), claustrum (CI), accumbens nucleus (Acb), caudate putamen (CPu), basolateral (BL) and central (Ce) divisions of amygdaloid nucleus, bed nucleus of the stria terminalis (STLD), ventral posterior division of the thalamic nucleus (VP), paraventricular hypothalamic nucleus (PVN), and arcuate hypothalamic nucleus (Arc). These activated regions likely form potential networks (indicated by dash lines) to influence physiological functions. A microscopic image shows an example of c-Fos expression (indicated by an arrow) in the Arc of a representative mouse following P6 acupuncture treatment.

Keywords

acupuncture; Fos; brain; sensory nerves; mouse genetics; RRID: MGI:5488917

1 INTRODUCTION

Acupuncture, including manual and electroacupuncture, is an important practice used in traditional Chinese medicine, and it generates therapeutic effects through the insertion of thin needles through the skin at specific acupoint(s) in the body to stimulate sensory nerves. Acupoints located along 12 bilaterally symmetrical meridians (overlying somatic neural pathways) serve as guides to properly insert acupuncture needles (Zhao. 2008; Hua. 1994). The World Health Organization lists over 40 conditions for which acupuncture may be useful, including, among others, pain and cardiovascular diseases (Longhurst. 2013; Langevin HM, Wayne PM, MacPherson H, et al. 2011; Goldman, Chen, Fujita T., et al. 2010). Acupuncture is used widely in the Eastern Asian and increasingly accepted as an effective and inexpensive medical alternative and complementary therapy for many diseases. A critical barrier for broader application of acupuncture outside of East Asia is the lack of mechanistic explanations of how it works. In particular, neural mechanisms by which acupuncture activates sensory nerves to regulate physiological function remain largely unknown. A detailed understanding of mechanisms underlying its action will promote the broader application of acupuncture to manage physiological disorders.

Acupuncture mechanistic studies in humans are complicated by the issue of patient expectations and placebo effects. Rodent models, however, allow for objective evaluations for acupuncture effects and neural mechanisms. Many of the acupoints have multiple therapeutic indications. For instance, the P6 acupoint overlying median nerve is used to treat cardiovascular diseases and nausea (Longhurst. 2013; Lv, Feng, & Li. 2013). In rodents, we have found that acupuncture applied at the Neiguan acupoint (P6) overlying the median nerve specifically modulates cardiovascular responses through influence on regions in the brainstem, including nucleus tractus solitarius, caudal and rostral ventrolateral medulla, raphe nuclei, as well as arcuate nucleus and paraventricular nucleus in the hypothalamus (Guo, Moazzami, & Longhurst. 2004; Li, Tjen-A-Looi, Guo, Fu, & Longhurst. 2009;

Longhurst. 2013). However, it is still unclear about neuronal activation in higher brain regions, in particular in the forebrain, by acupuncture at this acupoint. There is a critical need to determine the location of the neurons participating in the transmission and action of acupuncture in the central nervous system (CNS) so that neural circuits associated with neurons in the specific areas can be precisely targeted for acupuncture intervention.

Expression of c-Fos, an immediate early gene in neurons is a general marker for neuronal activation in response to specific stimulation (Guo, Li, & Longhurst. 2012; Guo, Moazzami, & Longhurst. 2004; Lee & Beitz. 1992; Lin, Itoga, Taha, et al. 2018). To reduce non-specific background, the current optimal identification of c-Fos is achieved in the Fos-CreER mice with tamoxifen-dependent recombinase CreER under the promoter of the immediate early gene c-Fos, crossed with the Cre reporter Ai9 mice to express tdTomato fluorescent protein (Figure 1) (Guenthner, Miyamichi, Yang, Heller, & Luo. 2013). This genetic method allows for enhanced sensitivity and efficiency compared to conventional immunohistochemical staining (Guenthner, Miyamichi, Yang, Heller, & Luo. 2013) along with temporal control of introducing stimulus after tamoxifen-CRE induction. In the present study, we used the Fos-CreER mouse generated in our local colony to map acupuncture-induced neuronal activation in higher brain regions throughout the forebrain and midbrain. We hypothesized that acupuncture at the P6 acupoint induces c-Fos expression in the multiple specific nuclei that form networks in higher brain regions beyond the brainstem.

2 MATERIALS AND METHODS

2.1 Animals

All experimental preparations and protocols were reviewed and approved by the Animal Care and Use Committee of the University of California at Irvine, CA and conform with National Institutes of Health guidelines for animal care and use. Studies were performed on young adult Fos-CreER; Ai9 mice (~10 weeks old) generated in our local mouse colony, which belong to C57BL/6 congenic strains, thus eliminating potential interpretational issues associated with comparison of different genetic backgrounds. The Fos-CreER; Ai9 mice are based on a cross between Fos-CreER mice with tamoxifen-dependent recombinase CreER under the promoter of the immediate early gene c-Fos and Cre reporter Ai9 mice that express the tdTomato fluorescent protein. Animals were group housed in standard conditions (temperature, 72° F; humidity, 40%) with a 12-hour light-dark cycle (lights on at 6:30 a.m., lights off at 6:30 p.m.).

2.2 Experimental Protocols

The Fos-CreER; Ai9 mice were randomly assigned to two groups, including acupuncture and sham-acupuncture ones. Anesthesia was induced with ketamine: xylazine (75:10 μg/g, i.m.). Additional doses of the anesthetics were given as necessary to maintain an adequate depth of anesthesia by observing the absence of conjunctival reflex response. At 30 min following the administration of the fast acting tamoxifen derivative, 4-Hydroxytamoxifen (4-OHT; 1 mg/per mouse, i.p.), manual acupuncture (MA) or sham-MA at P6 were conducted. The P6 acupoint is located on the forelimb 1.0 mm above the flexor crease in the paw overlying the median nerve (Figure 1) (Hua. 1994). MA (~2 Hz) applied at this acupoint

evokes median nerve discharge and attenuates reflex cardiovascular responses (Zhou, Fu, Tjen-A-Looi, Li, & Longhurst. 2005; Guo, Fu, Su, Tjen-A-Looi, & Longhurst. 2018). A stainless steel acupuncture needle (40-gauge, 0.16 mm × 15 mm) was inserted (2–3 mm) at P6. MA was performed bilaterally by gentle manual rotation of the acupuncture needle at a frequency of ~2 Hz for 3 min every 10 min during a 30 min period, closely mimicking the procedure as carried out in patients (Zhou, Fu, Tjen-A-Looi, Li, & Longhurst. 2005; Goldman, Chen, Fujita T., et al. 2010; Guo, Fu, Su, Tjen-A-Looi, & Longhurst. 2018). During sham-MA, the needle was inserted into the same acupoint without subsequent mechanical stimulation (Zhou, Fu, Tjen-A-Looi, Li, & Longhurst. 2005; Guo, Fu, Su, Tjen-A-Looi, & Longhurst. 2018). In previous studies, we have demonstrated that acupuncture at P6 has the specific action in modulating cardiovascular responses, compared to the insertion of acupuncture needle without stimulation as well as to acupuncture applied to other acupoints or non-acupoints in the forelimb (Longhurst & Tjen-A-Looi. 2013; Tjen-A-Looi, Li, & Longhurst. 2004; Li, Tjen-A-Looi SC., & Longhurst JC. 2013; Zhou, Fu, Tjen-A-Looi, Li, & Longhurst. 2005). Thus, in this study, we focused on investigating the specific activation of the forebrain areas by MA at P6 compared to the sham control in which the acupuncture needle was placed at the same acupoint without mechanical rotation. This sham control serves as an appropriate control for the experimental study of acupuncture (Langevin HM, Wayne PM, MacPherson H, et al. 2011). Correct placement of the needle at P6 was confirmed by observing slight repetitive paw twitches (indicating stimulation of motor fibers in median nerve) with electrical stimulation of P6 and P4 (an acupoint overlying median nerve 3.0 mm above the flexor crease).

The mice survived for ten days after administration of 4-OHT to allow sufficient tdTomato expression in Fos-positive neurons in the brain following MA or sham-MA. Afterward, mice were anesthetized deeply with isoflurane (inhalation). Transcardial perfusion was performed using 5 ml of 0.1 M phosphate buffered saline (PBS; pH 7.4) followed by 25 ml of 4% paraformaldehyde in PBS. Brain tissues were harvested and stored in 4% paraformaldehyde overnight, then stored in 30% sucrose at 4 °C to prevent ice crystallization until cutting. Coronal sections of the brain (30 μm) were made with a freezing microtome collected serially in cold cryoprotectant solution. Brain sections were mounted on microscope slides in PBS. The slides were allowed to air-dry overnight, then covered by glass slips with permount (Fisher Scientific, Fair Lawn, New Jersey, USA).

2.3 Data analysis

Brain sections were scanned and examined with a 10× objective of a fluorescent microscope (Olympus BX 61) equipped with a high-sensitive CCD camera and Metamorph software for brain-wide analysis of labeled tissue. The epi-fluorescence narrow-band green filter equipped in a fluorescent microscope is optimized for detection of a single stain appearing as red (tdTomato). It was used to identify c-Fos expression in the brain sections. Consistent with published studies (Guenthner, Miyamichi, Yang, Heller, & Luo. 2013), the Fos positive neurons were readily visualized with native fluorescence from genetic tdTomato expression in the Fos-Cre; Ai9 mice. The c-Fos positive cells appeared as a red round dot of about 7–12 μm in diameter and were distinguishable from background staining at 40× magnification. Images were obtained using the Metamorph image acquisition software (Molecular Devices,

Sunnyvale, CA), and analysis was done using Adobe Photoshop (CS4). Slice images were overlaid with corresponding maps of Franklin & Paxinos's atlas for the mouse (Franklin & Paxinos, 2007) to confirm the identity of different brain regions. Once the area was measured, Fos-positive neurons were counted manually using a Photoshop counting tool.

After examining many brain sections in each case, we selected 13 representative sections for cell counting analysis, which included all primary nuclei or their divisions located in the forebrain and midbrain regions. These selected sections most closely match the standard stereotaxic planes of Franklin & Paxinos's atlas for the mouse (Franklin & Paxions. 2007), as shown in Figure 4. One representative section, including both hemispheres in each plane was evaluated from each mouse. The c-Fos positive neurons were counted in unbiased selected brain sections in two groups. The counting was conducted by laboratory staff with treatment information blind to them. The number of single Fos-positive cell was counted bilaterally in each animal. The average number of the Fos-positive cells in two or three representative levels taken from the rostro-caudal extension of each nucleus in the forebrain was calculated by dividing the total number of the cells by the number of the representative levels, thus representing the number of sections used for cell counting.

2.4 Statistical analyses:

Data were expressed as means ± SE and considered to be significantly different as $P<0.05$. We used the Kolmogorov–Smirnoff test to determine if the data were normally distributed. Comparisons between two groups were statistically analyzed with the Student's t-test or Mann–Whitney rank sum test. To analyze the linear relationship of Fos-activation among brain regions induced by acupuncture, we calculated pair-wise Pearson correlation coefficients (r), correlating numbers of Fos-positive cells within each area to other ones. All statistical calculations were performed with a statistical software package (SigmaStat, Version 3.0, Jandel Scientific Software, San Rafael, CA, USA).

3 RESULTS

The c-Fos expression in the neuron, appearing as red dots, is found bilaterally in many regions across the forebrain in the mice subjected to sham-MA (n=5, Figure 2) or MA (n=5, Figure 3). Each figure includes original images showing 13 forebrain tissue slices from rostral to caudal levels selected from one mouse in each group. The 13 slices represent sections from Bregma 2.96, 2.22, 1.54, 0.86, 0.14, −0.58, −0.82, −1.34, −2.06, −2.80, −3.52, −4.24, and −4.96 mm with 0.68 – 0.72 mm intervals. The ranges between segments at the levels of Bregma from −0.58 to −0.82 mm and from −0.82 to −1.34 mm are 0.24 and 0.52 mm, respectively. The section at Bregma −0.82 mm is selected specifically because this segment contains a significant portion of the PVN. These selected sections are closely matched to corresponding levels of Bregma of the forebrain, which are demonstrated in the Franklin & Paxinos mouse brain atlas (Franklin & Paxions. 2007) as well as in Figure 4 which schematically depicts Fos-positive cells to brain regions. As shown in Figures 2–4, the selected sections include all nuclei or their divisions located in the forebrain and midbrain regions. Those regions excluded contain small nuclei in the thalamus, hypothalamus, and midbrain, as well as minor commissural or tract nuclei such as the

precommissural nucleus, scaphoid nucleus, circular nucleus, stigmoid nucleus, premammillary nucleus, and the fields of Forel, among others. In those areas, no or scarce c-Fos positive neurons are found similarly in both sham-MA and MA group. Thus, they are not displayed in the figures.

We systematically examine c-Fos expression at the multiple rostro-caudal levels noted above, according to the mouse brain atlas (Franklin & Paxions. 2007). We identify a notable significant increase in c-Fos positive neurons in some specific nuclei of the forebrain in mice treated with MA, described in detail below, compared to sham-MA (Figures 2–4 and Table 1). We also find that there is no significant difference in the number of Fos-positive cells between the two groups in the majority of forebrain regions (Table 1).

In the cortex, significant increases in c-Fos expression ($p<0.05$) are observed in the mice treated with MA in the somatosensory cortices (S), including primary (S1) and secondary (S2) somatosensory cortex, ectorhinal cortex (Ect), and dorsolateral entorhinal cortex (DLEnt), compared to control mice (Table 1 and Figure 4). In the MA-treated mice, c-Fos expression density in the S tends to be much higher at the rostral levels (Bregma 0.86 through −0.82 mm), followed by a decrease with more caudal levels (Figure 4). In the Ect, more c-Fos expression is observed rostrally but Ect Fos expression decreases when approaching the midbrain (Figure 4, Bregma −1.34 through −4.96 mm). Unlike the expression observed in the Ect, the majority of Fos expression in the DLEnt, positioned just below the Ect, are found in sections closer to the midbrain (Figure 4, Bregma −2.06 through −2.80 mm). Although Fos-positive neurons are identified in the majority of cortex regions, there is no significant difference in the number of these neurons between sham-MA and MA groups. These areas include the visual cortex, frontal association cortex, area 3 of the frontal cortex, motor cortices, areas 1 and 2 of the cingulate cortex, the prelimbic and infralimbic cortices, the dorsal tenia tecta, the piriform cortex, the insular cortices, retrosplenial cortices, the perirhinal cortex, parietal cortices, the temporal association cortex, the presubiculum postsubiculum, and transition area of the subiculum (Table 1).

We find c-Fos positive neurons in the basal nuclei in both groups. However, the number of cells expressing c-Fos (about 18 cells per section) in the claustrum (CI) of MA-treated mice is three times more than that in the mice subjected to sham-MA, in which few cells (approximate 6 cells per section) expressing c-Fos are found (Figure 4, Bregma 1.54 through −0.82 mm). Fos-positive neurons are increased significantly in the accumbens nucleus (Acb) of MA-treated mice in comparison with sham-MA mice ($p<0.05$; Table 1). Most c-Fos expression is observed in the shell of the Acb with scattered expression within its core. Despite the presence of c-Fos expression throughout the caudate putamen (CPu) of all mice in two groups, there are more (slightly over double) neurons expressing c-Fos in MA-treated mice than those in mice that underwent sham-MA (Figure 4, Bregma 1.54 through −1.34 mm).

The amygdala nucleus includes the central division (Ce) and basolateral division (BL). C-Fos expression is found more frequently in this nucleus, particularly in the Ce of MA-treated mice, compared to mice that underwent sham-MA (Figures 2 and 3). There is 24 times more c-Fos expression identified in the Ce of mice with MA treatment than that in sham-MA

controls ($p<0.05$; Table 1, Figure 4, Bregma −0.58 through −2.06 mm). The Fos-positive cells are located mainly in the medial and central parts of the Ce (Figure 4). In the BL, c-Fos expression is not increased as dramatically as that in the Ce. However, there is a significant difference between the two groups ($p<0.05$; Table 1 and Figure 4, Bregma −0.58 through −2.06 mm).

In the bed nucleus of the stria terminalis (BNST), the most expression of c-Fos is identified in the lateral division of BNST (STLD), particularly in the dorsal part of STLD in MA-treated mice. In contrast, very few neurons expressing c-Fos are found in the mice that underwent sham-MA (Figures 2 and 3, and Figure 4, Bregma 0.14 mm). There is a significant difference in the number of Fos-positive cells between these two groups ($p<0.05$; Table 1). Such prominent expression of c-Fos is not noted in the other parts of the BNST in mice treated with MA or sham-MA.

We observe, in the thalamus, a significant increase in c-Fos expression primarily in its ventral posterior division (VP) of the mice subjected to MA treatment, compared to sham-MA controls ($p<0.05$; Table 1 and Figure 4, Bregma −1.34 through −2.06 mm). The expression of c-Fos is identified in the lateral and medial portions of the VP (Figure 4). Less c-Fos positive cells are noted in the lateral parts of the VP (VPL) than those in the medial part of the VP (VPM) in both MA and sham-MA groups. However, importantly, the c-Fos positive cells are significantly increased in VPL but not in VPM in MA-treated mice, in comparison with controls. Besides, there is no significant difference between the two groups (Table 1) in the number of Fos-positive neurons in the ventrolateral, ventromedial, mediodorsal, central medial, and submedius divisions of the thalamic nucleus, and neither in the paratenial thalamic nucleus and habenular nucleus.

In the hypothalamus, a marked increase in c-Fos expression is located in the paraventricular nucleus (PVN) and arcuate nucleus (Arc) in the mice treated with MA, compared to sham-MA controls ($p<0.05$; Table 1, Figures 2–4). Notably, we only find very few Fos-positive neurons (about one cell per section) in the PVN of mice underwent sham-MA. In contrast, about 13 Fos-positive neurons per section are identified in MA-treated mice (Figures 2–4, Bregma −0.82 mm). In the Arc nucleus, while there are some Fos-positive cells noted in the mice treated with sham-MA, obviously more c-Fos expression is observed in MA-treated mice, especially approaching the level at Bregma −2.06 mm as shown in Figures 2–4.

We note that in the areas of the midbrain, excluding the aforementioned cortex regions, there is no significant difference in c-Fos expression between MA-treated group and control group (Table 1). Notably, in the periaqueductal gray (PAG), we observe c-Fos expression primarily located in its lateral portions, with no or little presence in its dorsal parts, approaching the level at Bregma −4.24 mm in both groups.

Among all regions in which more c-Fos expression is found in MA-treated mice than in controls, there are significant correlations of the numbers of Fos-positive neurons between some nuclei following MA treatment, including PVN and STLD, S and CI, CI and Arc, as well as Ect and STLD (Table 2 and Figure 5).

4 DISCUSSION

In the present study, we examined P6 acupuncture-specific neural activation in the forebrain using a Fos-CreER based mouse genetic strategy, a robust and sensitive genetic method to identify the activation of the central neurons. We visualized and identified neurons activated by MA applied at P6 in the forelimb within multiple specific regions in the forebrain relative to sham controls, including S, Ect, DLEnt, Cl, Acb, CPu, Ce, BL, BNST, VP, PVN, and Arc. These results support our hypothesis and provide new evidence showing unique nuclei activated during acupuncture applied at a specific acupoint like P6. Thus, the present study helps us understand the fundamental concepts of long-range input and output connections of neurons in the context of acupuncture, which is helpful for us to identify neural circuit components for acupuncture intervention.

Acupuncture presents as a non-pharmacological option to treat many diseases. Potential advantages of acupuncture over conventional medical therapy include its prolonged action and few, if any, of side effects (Longhurst. 2013). It can be a viable, inexpensive alternative or complementary to conventional therapies with prolonged action. Although acupuncture has been used for centuries, mechanistic evidence of its effects is still lacking. The critical barrier to employment of acupuncture clinically is a lack of detailed understanding of its mechanisms. Acupuncture signals begin in the periphery and ascend to higher central brain areas (Zhou, Fu, Tjen-A-Looi, Li, & Longhurst. 2005; Zhou, Tjen-A-Looi, & Longhurst JC. 2005; Zhao. 2008). We have studied acupuncture's cardiovascular effects and found that acupuncture applied at the P6 acupoint overlying somatic median nerve attenuates elevation in blood pressure through modulation of the activity in multiple regions in the brainstem, for instance, the rostral ventrolateral medulla (rVLM) that critically controls sympathetic outflow to regulate cardiovascular function (Zhou, Tjen-A-Looi, & Longhurst JC. 2005; Li, Tjen-A-Looi, Guo, Fu, & Longhurst. 2009; Longhurst. 2013). Besides treating cardiovascular diseases, acupuncture at P6 is also used to manage other clinical disorders, like nausea (Lv, Feng, & Li. 2013; Longhurst. 2013). It remains unclear about brain regions beyond the brainstem activated by acupuncture at this acupoint and their correlations. The forebrain plays an essential role in the integration of sensory inputs and processing neural regulation of physiological function (Dampney. 1994). Thus, in the present study, we systemically identified specific locations of the neurons and neural circuits in the forebrain in response to acupuncture stimulation at the P6 acupoint.

The connection between the expression of immediate early genes such as c-Fos and neuronal responses is well established (Krukoff. 1998; Morgan, Cohen, Hempstead, & Curran. 1987). The c-Fos expression is low in quiescent cells but can be induced rapidly and transiently by sensory stimuli (Krukoff. 1998; Morgan, Cohen, Hempstead, & Curran. 1987). Identification of activated neurons with their c-Fos expression in the brain following acupuncture has been studied with conventional Fos immunochemical staining in other species (e.g., rats and cats) (Guo, Li, & Longhurst. 2012; Guo, Moazzami, & Longhurst. 2004; Lee & Beitz. 1992). In the present study, we used technological advancements in genetic cell targeting to determine detailed neural activation patterns related to acupuncture's action within the forebrain. The Fos-CreER mouse with tamoxifen-dependent recombinase CreERT2 under the c-Fos promoter is crossed to a Cre reporter Ai9 mouse line to generate c-Fos CreER; Ai9 mouse to

express tdTomato FP in Fos active neurons under the control of administration tamoxifen or its metabolite 4-OHT (Guenthner, Miyamichi, Yang, Heller, & Luo. 2013) (Figure 1). The lifetime of tamoxifen is limited by metabolism. Compared to tamoxifen, injecting 4-OHT shortens Cre-recombination time window (i.e., a few hours) and thus reduces the integration of activity over a shorter period of time as compared with tamoxifen injection. As such, 4-OHT was used in the present study. This genetic strategy takes advantage of regulatory elements of c-Fos to express a tamoxifen-dependent recombinase, CreERT2 in an activity-dependent manner (Guenthner, Miyamichi, Yang, Heller, & Luo. 2013). The genetic labeling method is more sensitive and robust than conventional c-Fos expression mapping and shows less non-specific background. The activated neurons expressing c-Fos following stimulation were permanently labeled with tdTomato FP expression appearing as bright red fluorescence that does not require immuno-enhancement for detection. This state-of-art method has been used for mapping neuronal activities based on their genetic identities (Guenthner, Miyamichi, Yang, Heller, & Luo. 2013). Consistent with previously published work (Guenthner, Miyamichi, Yang, Heller, & Luo. 2013), we captured active neuronal populations in response to MA at P6 using this approach in the Fos-CreER; Ai9 mice within a limited time window of 4-OHT injection (30 min). The neurons expressing c-Fos following MA are likely associated with MA's transmission and modulation, as compared to sham-operated MA controls, in which the same procedures as MA were performed except for no manual mechanical stimulation. As such, in the present study, the increase in genetic labeling obtained in the adopted model of Fos-CreER; Ai9 mice is likely due to c-Fos mediated activation in the brain in response to acupuncture.

The Fos population can be unambiguously identified since the Fos is uniquely expressed. In the present study, as the number of Fos in specified areas across the forebrain was quantitatively determined, our measurements enabled quantitative assessment of the relative abundance of neuronal populations in response to MA at P6. This quantification helped us to answer the proposed questions of whether the input from the P6 acupoint was distributed in the specific forebrain regions and different strengths onto the physiological-regulated areas. In this regard, we observed that increase in c-Fos expression in some particular regions in the cortex, thalamus, and hypothalamus, which are known to play an essential role in central processing of sensory inputs and regulate neural activity.

In the cortex, a pronounced increase for P6 MA evoked c-Fos expression was observed in the S, Ect, and DLEnt in the present study. The most significant increase was seen in the S, including S1 and S2 in MA-treated mice. It is likely due to brain reactions in responses to sensory afferent inputs generated by manual rotation of needle at the P6 acupoint. With this respect, our previous studies have demonstrated that MA at P6 stimulates myelinated and unmyelinated nerve fibers that are richly present at the acupoint and then activates sensory neurons in dorsal root ganglia, which lead to transmitting neural signals to the brain (Guo, Fu, Su, Tjen-A-Looi, & Longhurst. 2018). It is known that somatic nerve inputs travel through thalamocortical projections from the ventral posterior thalamic nucleus (VP) and then relay the information to S1 and S2 (Vierck, Whitsel, Favorov, Brown, & Tommerdahl. 2013). The S2 (association cortices) integrate sensory input responses from the S1. This integration serves a variety of functions, including recognition of the stimulus. The S2 may also be involved in motor planning and modulation of sensory impulses. The Ect and DLEnt

are interconnected and located in ventromedial temporal cortical regions, and they contain sympathetic-related neurons. Both of them receive inputs from the S, and are part of cortico-cortical circuits that process higher-level brain functions such as memory, navigation, perception, and modulation of sympathetic responses (Eichenbaum, Yonelinas, & Ranganath. 2007; Westerhaus & Loewy. 2001). Notably, the DLEnt innervates the amygdala that is linked multisynaptically to the sympathetic nervous system. It also may bypass the amygdala to project directly or indirectly to sympathetic-related neurons in the hypothalamic area (Westerhaus & Loewy. 2001). Given the fact of involvement of the cortex in regulation of a variety of activities, including autonomic functions, the activation of these cortical areas by MA is suggestive of their participations in central processing of the action of MA at P6, particularly a potential modulation of the sympathetic outflows associated with cardiovascular system. Likely, these cortical areas do not project directly to sympathetic preganglionic neurons in the spinal cord, but they are part of multi-synaptic circuits that have relays to the hypothalamus and/or brainstem.

The CI, CPu, Acb, and amygdala are components of the basal nuclei. The CI forms extensive reciprocal connections with almost all regions of the cortex, as well as subcortical structures such as CPu, the amygdala, and thalamus. It might be involved in the integration of sensory information through interactions with multiple brain regions (Crick & Koch. 2005; Wang, Ng, Harris, et al. 2017). Both CPu and Acb receive inputs from the cortex and sending outputs to the thalamus and hypothalamus (Haber. 2016; Heimer, Zahm, Churchill, Kalivas, & Wohltmann. 1991; Benarroch. 1993). Besides involvement in motor functions, these two nuclei also play a role in the regulation of emotional behavior, cognition, and autonomic functions (Haber. 2016; Schlindwein, Buchholz, Schreckenberger, Bartenstein, Dieterich, & Birklein. 2008). Electrical stimulation of the CPu and Acb causes changes in blood pressure, heart rate, and respiratory rate (Angyan. 1994). Moreover, the CPu functions as a part of the central autonomic network involved in vagal control (Wei, Chen, & Wu. 2018). The amygdala is a primary structure of the central autonomic network (Dampney. 1994) in addition to playing a role in modulation of emotional responses (Rasia-Filho, Londero, & Achaval. 2000; Wei, Chen, & Wu. 2018). Notably, it contributes to cardiovascular regulation through its input and output connections to other central autonomic control regions, including the cortex, hypothalamus, and brainstem (Hopkins & Holstege. 1978). Previous studies have shown that its central division (Ce) is involved in modulation of cardiovascular function, likely through the mediation of the parasympathetic outflow (Roozendaal, Koolhaas, & Bohus. 1991), and its basolateral division (BL) is mainly activated in response to psychological stressors (al Maskati & Zbrozyna. 1989). Moreover, Zhao and colleagues have shown that MA at P6 ameliorates acute restraint stress through influence on the Ce and BL (Zhao, Kim, Liu, et al. 2017). The BNST is considered as the extended amygdala and serves a key relay connecting limbic forebrain structures to hypothalamic and brainstem regions. This nucleus is involved in central autonomic regulation (Crestani, Alves, Gomes, Resstel, Correa, & Herman. 2013; Rasia-Filho, Londero, & Achaval. 2000; Ciriello & Janssen. 1993), particularly, amygdala-mediated cardiovascular reactions (Roder & Ciriello. 1993). In the present study, we found that MA at P6 induces a significant increase in c-Fos expression in CI, CPu, Acb, BNST, and the amygdale, especially in its Ce and BL divisions. Our results suggest that these basal nuclei

are involved in central processing MA's action in regulating cardiovascular and other autonomic functions through neural networks among them and their direct or indirect connections to nuclei in the cortex, hypothalamus and brainstem.

The thalamus is well known as a relay center for sensory information, with pathways to and from the cortex, subcortical areas, and the brainstem. Among multiple thalamic subdivisions responsible for sensory, motor and cognitive functions differently, the VP mainly receives neuronal input from spinothalamic tracts, and projects to the S. In the present study, we found that MA at P6 increases c-Fos expression in the VP, particularly in its lateral part that processes sensory information from the body including the forelimb where P6 is located. Thus, our findings suggest that neural signals induced by MA at P6 input to VP that relays the information to the S, which form relative specific spinothalamic pathway conveying afferent sensory information from MA.

The hypothalamus is an essential region in regulating autonomic and endocrine function and maintaining homeostasis (Bouret, Draper, & Simerly. 2004; Elmquist, Elias, & Saper. 1999; Rahmouni. 2016). In the present study, we found that MA at P6 causes a significant increase in c-Fos expression in two hypothalamic nuclei, PVN, and Arc. The PVN receives afferent inputs from many brain regions, including amygdala, BNST, Arc, and among others (Westerhaus & Loewy. 2001; Bouret, Draper, & Simerly. 2004; Radley & Johnson. 2018). While the PVN is one of the primary sources of inputs to sympathetic preganglionic neurons in the spinal cord, it also projects to the cortex and innervates other autonomic nuclei in the brainstem, which in turn influences autonomic nerve activity (Dampney. 1994). Besides involvement in the metabolic regulation, the Arc has cardiovascular implications (Bouret, Draper, & Simerly. 2004; Rahmouni. 2016). This action likely occurs through Arc's direct influence on multiple cardiovascular-related nuclei, such as the PVN and rVLM (Bouret, Draper, & Simerly. 2004; Rahmouni. 2016; Kawabe, Kawabe, & Sapru. 2012; Li, Tjen-A-Looi, Guo, Fu, & Longhurst. 2009). Our previous studies have shown that both PVN and Arc are involved in modulation of sympathoexcitaory cardiovascular reflexes by EA applied at the Jianshi (P5) and P6 acupoints (Li, Tjen-A-Looi, Guo, Fu, & Longhurst. 2009; Tjen-A-Looi, Guo, Fu, & Longhurst. 2016). In the present study, our observation of activated neurons in these nuclei following MA at P6 implies potential contributions of the PVN and Arc to MA's regulation of cardiovascular responses.

On the whole, our results show that MA at P6 activates several specific areas in the forebrain, which have aforementioned direct or indirect connections and form neural networks to process MA's inputs and subsequent responses. The activated regions likely are involved directly or indirectly in the regulation of autonomic function, including cardiovascular responses. In this respect, our data suggest potential long-range input and output pathways from the peripheral sensory afferents stimulated by acupuncture to the brain nuclei that are responsible for the regulation of hemostasis, especially for the autonomic function. Specifically, MA at P6 likely activates sensory afferents and sends inputs to VP through spinothalamic tracts, which then projects to S. The neural signals received by S are integrated with this area and transmitted to other cortical nuclei, like Ect and DLEnt. The neural impulses from the cortex project to the basal nuclei, including Cl, Acb, CPu, amygdala, and BNST, which influence hypothalamic Arc and PVN. Finally, the

hypothalamic nuclei regulate sympathetic and parasympathetic outflows through their direct or indirect connections to the brainstem and spinal cord (Dampney. 1994). Thus, the data from the present study provide further evidence to elucidate central neural mechanisms by which MA at P6 modulates cardiovascular responses, as we have demonstrated previously. Our new findings advance our knowledge about neuronal activation induced by MA at P6 in the forebrain, which contributes to the organization of central neural circuits particularly involved in cardiovascular control. It helps establish a mechanistic framework to account for P6-specific effects on the CNS and our broad and deep understanding of acupuncture's action at P6. Moreover, our results suggest a larger scale mechanistic investigation related to acupuncture's effect, which will contribute to the development of more specific and practical strategies for application of acupuncture.

Although we operationally define acupuncture-activated neurons as Fos-expressing neurons, it is possible that activated neurons following acupuncture include "acupuncture-specific" neurons and other "non-specific" neurons. The latter neurons may comprise those activated in normal physiological processes or those indirectly activated by acupuncture, which is not a direct part of circuits involving in acupuncture action. This limitation of specificity needs to be overcome in future studies with new technological developments. Besides, future studies also will be required to confirm and validate genetic capture of acupuncture-activated specific neurons by testing its influence on the activity of neurons that control physiological function, for instance, cardiovascular function.

In summary, the present study used recently developed techniques (genetic cell targeting) to elucidate neuronal activation by acupuncture. We first established the genetic approach for visualizing acupuncture-activated neurons by their c-Fos expressions, with a scientific goal of creating cellular details of acupuncture-activation in the specific brain regions. Results from the present study more clearly answer essential questions about brain responses to acupuncture, which extend our knowledge of acupuncture's action on CNS. Thus, the anatomical findings allow for a fundamental understanding of large-scale input and output neurons in the context of acupuncture modulation of physiological function, and they will guide functional studies.

ACKNOLEDGMENTS

This study was supported by NCCIH AT009347 (Z Guo and S Malik) and diversity supplement award to this grant (T Samaniego), NIH MH113026 (X Xu) and GM127102 (T. C. Holmes).

Abbreviations

4-OHT	4-Hydroxytamoxifen
Acb	Accumbens nucleus
Arc	Arcuate nucleus
BL	Basolateral division of the amygdaloid nucleus
BNST	Bed nucleus of the stria terminalis

Ce	Central division of amygdaloid nucleus
Cl	Claustrum
CM	Central medial division of the thalamic nucleus
CPu	Caudate putamen
CNS	Central nervous system
DLEnt	Dorsolateral entorhinal cortex
Ect	Ectorhinal cortex
MA	Manual acupuncture
P6	Neiguan acupoint
PAG	Periaqueductal gray
PVN	Paraventricular nucleus
rVLM	Rostal ventrolateral medulla
S	Primary and secondary somatosenseory cortices
STLD	Lateral division of the BNST, dorsal part
VP	Ventral posterior division of the thalamic nucleus

Reference List

al Maskati HA, & Zbrozyna AW (1989). Cardiovascular and motor components of the defence reaction elicited in rats by electrical and chemical stimulation in amygdala. J Auton.Nerv.Syst, 28, 127–131. [PubMed: 2625501]

Angyan L. (1994). Somatomotor and cardiorespiratory responses to basal ganglia stimulation in cats. Physiol Behav, 56, 167–173. [PubMed: 8084896]

Benarroch EE (1993). The central autonomic network: functional organization, dysfunction, and perspective. Mayo Clin.Proc, 68, 988–1001. [PubMed: 8412366]

Bouret SG, Draper SJ, & Simerly RB (2004). Formation of projection pathways from the arcuate nucleus of the hypothalamus to hypothalamic regions implicated in the neural control of feeding behavior in mice. J Neurosci, 24, 2797–2805. [PubMed: 15028773]

Ciriello J, & Janssen SA (1993). Effect of glutamate stimulation of bed nucleus of the stria terminalis on arterial pressure and heart rate. Am J Physiol, 265, H1516–H1522 [PubMed: 7902013]

Crestani CC, Alves FH, Gomes FV, Resstel LB, Correa FM, & Herman JP (2013). Mechanisms in the bed nucleus of the stria terminalis involved in control of autonomic and neuroendocrine functions: a review. Curr.Neuropharmacol, 11, 141–159. [PubMed: 23997750]

Crick FC, & Koch C. (2005). What is the function of the claustrum? Philos.Trans.R.Soc.Lond B Biol.Sci, 360, 1271–1279. [PubMed: 16147522]

Dampney RAL (1994). Functional organization of central pathways regulating the cardiovascular system. Physiol.Rev, 74, 323–364. [PubMed: 8171117]

Eichenbaum H, Yonelinas AP, & Ranganath C. (2007). The medial temporal lobe and recognition memory. Annual Review of Neuroscience, 30, 123–152.

Elmquist JK, Elias CF, & Saper CB (1999). From lesions to leptin: hypothalamic control of food intake and body weight. Neuron, 22, 221–232. [PubMed: 10069329]

Franklin KBJ, & Paxions G. (2007). The mouse brain in stereotaxic corrdinates. New York: Academic Press.

Goldman N, Chen M, Fujita T, Xu Q, Peng W, Liu W, Jensen T, Pei Y, Wang FHX, Chen J, Schnermann J, Takano T, Bekar L, Tieu K, & Nedergaard M. (2010). Adenosine A1 receptors mediate local anti-nociceptive effects of acupuncture. Nat Neurosci, 13, 883–888. [PubMed: 20512135]

Guenthner CJ, Miyamichi K, Yang HH, Heller HC, & Luo L. (2013). Permanent genetic access to transiently active neurons via TRAP: targeted recombination in active populations. Neuron, 78, 773–784. [PubMed: 23764283]

Guo Z-L, Li M, & Longhurst J. (2012). Nucleus ambiguus cholinergic neurons activated by acupuncture: relation to enkephalin. Brain Research, 1442, 25–35. [PubMed: 22306033]

Guo Z-L, Moazzami AR, & Longhurst JC (2004). Electroacupuncture induces c-Fos expression in the rostral ventrolateral medulla and periaqueductal gray in cats: relation to opioid containing neurons. Brain Research, 1030, 103–115. [PubMed: 15567342]

Guo ZL, Fu LW, Su HF, Tjen-A-Looi SC, & Longhurst JC (2018). Role of TRPV1 in acupuncture modulation of reflex excitatory cardiovascular responses. Am J Physiol Regul Integr Comp Physiol, 314, R655–R666 [PubMed: 29351423]

Haber SN (2016). Corticostriatal circuitry. Dialogues.Clin.Neurosci, 18, 7–21. [PubMed: 27069376]

Heimer L, Zahm DS, Churchill L, Kalivas PW, & Wohltmann C. (1991). Specificity in the projection patterns of accumbal core and shell in the rat. Neuroscience, 41, 89–125. [PubMed: 2057066]

Hopkins DA, & Holstege G. (1978). Amygdaloid projections to the mesencephalon, pons and medulla oblongata in the cat. Exp.Brain Res, 32, 529–547. [PubMed: 689127]

Hua XB (1994). Acupuncture manual for small animals In Anonymous, Experimental acupuncture. (pp. 269–290). Shanghai, China: Shanghai Science and Technology Publisher.

Kawabe T, Kawabe K, & Sapru HN (2012). Cardiovascular responses to chemical stimulation of the hypothalamic arcuate nucleus in the rat: role of the hypothalamic paraventricular nucleus. PLoS.One, 7, e45180 [PubMed: 23028831]

Krukoff T. (1998). c-Fos expression as a marker of functional activity in the brain: immunohistochemistry In Boulton ABGBA (Ed.), Cell Neurobiology Techniques. Neuromethods (Vol. 33). (pp. 213–230). Humana, Bateson.

Langevin HM, Wayne PM, MacPherson H, Schnyer R, Milley RM, Napadow V, Lao L, Park J, Harris RE, Cohen M, Sherman KJ, Haramati A, & Hammerschlag R. (2011). Paradoxes in acupuncture research: strategies for moving forward. Evid Based Complement Alternat Med, 180805, 1–11.

Lee JH, & Beitz AJ (1992). Electroacupuncture modifies the expression of c-fos in the spinal cord induced by noxious stimulation. Brain Res, 577, 80–91. [PubMed: 1521149]

Li P, Tjen-A-Looi SC, & Longhurst JC. (2013). Acupuncture's role in cardiovascular homeostasis In Xia Ying, Dong Guanghong, & Wu Gen-Cheng (Eds.), Current Research in Acupuncture. (pp. 457–486). New York: Springer Science+Business Media.

Li P, Tjen-A-Looi SC, Guo ZL, Fu L-W, & Longhurst JC (2009). Long-loop pathways in cardiovascular electroacupuncture responses. Journal of Applied Physiology, 106, 620–630. [PubMed: 19074569]

Lin X, Itoga CA, Taha S, Li MH, Chen R, Sami K, Berton F, Francesconi W, & Xu X. (2018). c-Fos mapping of brain regions activated by multi-modal and electric foot shock stress. Neurobiol.Stress, 8, 92–102. [PubMed: 29560385]

Longhurst J. (2013). Acupuncture's Cardiovascular Actions: A Mechanistic Perspective. Med.Acupunct, 25, 101–113. [PubMed: 24761168]

Longhurst JC, & Tjen-A-Looi SC (2013). Acupuncture regulation of blood pressure: two decades of research. Int.Rev.Neurobiol, 111, 257–271. [PubMed: 24215927]

Lv JQ, Feng RZ, & Li N. (2013). P6 acupoint stimulation for prevention of postoperative nausea and vomiting in patients undergoing craniotomy: study protocol for a randomized controlled trial. Trials, 14, 153 [PubMed: 23710881]

Morgan JI, Cohen DR, Hempstead JL, & Curran T. (1987). Mapping patterns of c-fos expression in the central nervous system after seizure. Science, 237, 192–197. [PubMed: 3037702]

Radley JJ, & Johnson SB (2018). Anteroventral bed nuclei of the stria terminalis neurocircuitry: Towards an integration of HPA axis modulation with coping behaviors - Curt Richter Award Paper 2017. Psychoneuroendocrinology, 89, 239–249. [PubMed: 29395488]

Rahmouni K. (2016). Cardiovascular Regulation by the Arcuate Nucleus of the Hypothalamus: Neurocircuitry and Signaling Systems. Hypertension, 67, 1064–1071. [PubMed: 27045026]

Rasia-Filho AA, Londero RG, & Achaval M. (2000). Functional activities of the amygdala: an overview. J Psychiatry Neurosci, 25, 14–23. [PubMed: 10721680]

Roder S, & Ciriello J. (1993). Contribution of bed nucleus of the stria terminalis to the cardiovascular responses elicited by stimulation of the amygdala. J Auton.Nerv.Syst, 45, 61–75. [PubMed: 8227965]

Roozendaal B, Koolhaas JM, & Bohus B. (1991). Central amygdala lesions affect behavioral and autonomic balance during stress in rats. Physiol Behav, 50, 777–781. [PubMed: 1775553]

Schlindwein P, Buchholz HG, Schreckenberger M, Bartenstein P, Dieterich M, & Birklein F. (2008). Sympathetic activity at rest and motor brain areas: FDG-PET study. Auton.Neurosci, 143, 27–32. [PubMed: 18723403]

Tjen-A-Looi SC, Guo ZL, Fu LW, & Longhurst JC (2016). Paraventricular Nucleus Modulates Excitatory Cardiovascular Reflexes during Electroacupuncture. Sci.Rep, 6, 25910 [PubMed: 27181844]

Tjen-A-Looi SC, Li P, & Longhurst JC (2004). Medullary substrate and differential cardiovascular response during stimulation of specific acupoints. Am J Physiol, 287, R852–R862

Vierck CJ, Whitsel BL, Favorov OV, Brown AW, & Tommerdahl M. (2013). Role of primary somatosensory cortex in the coding of pain. Pain, 154, 334–344. [PubMed: 23245864]

Wang Q, Ng L, Harris JA, Feng D, Li Y, Royall JJ, Oh SW, Bernard A, Sunkin SM, Koch C, & Zeng H. (2017). Organization of the connections between claustrum and cortex in the mouse. J Comp Neurol, 525, 1317–1346. [PubMed: 27223051]

Wei L, Chen H, & Wu GR (2018). Heart rate variability associated with grey matter volumes in striatal and limbic structures of the central autonomic network. Brain Research, 1681, 14–20. [PubMed: 29278717]

Westerhaus MJ, & Loewy AD (2001). Central representation of the sympathetic nervous system in the cerebral cortex. Brain Research, 903, 117–127. [PubMed: 11382395]

Zhao Z, Kim SC, Liu H, Zhang J, Wang Y, Cho IJ, Lee BH, Song CH, Lee CW, Yang CH, Zhao R, & Wu Y. (2017). Manual Acupuncture at PC6 Ameliorates Acute Restraint Stress-Induced Anxiety in Rats by Normalizing Amygdaloid Noradrenergic Response. Evid.Based.Complement Alternat.Med, 2017, 4351723 [PubMed: 28900460]

Zhao ZQ (2008). Neural mechanism underlying acupuncture analgesia. Prog.Neurobiol, 85, 355–375. [PubMed: 18582529]

Zhou W, Fu L-W, Tjen-A-Looi SC, Li P, & Longhurst JC (2005). Afferent mechanisms underlying stimulation modality-related modulation of acupuncture-related cardiovascular responses. J Appl Physiol, 98, 872–880. [PubMed: 15531558]

Zhou W, Tjen-A-Looi S, & Longhurst JC. (2005). Brain stem mechanisms underlying acupuncture modality-related modulation of cardiovascular responses in rats. Journal of Applied Physiology, 99, 851–860. [PubMed: 15817715]

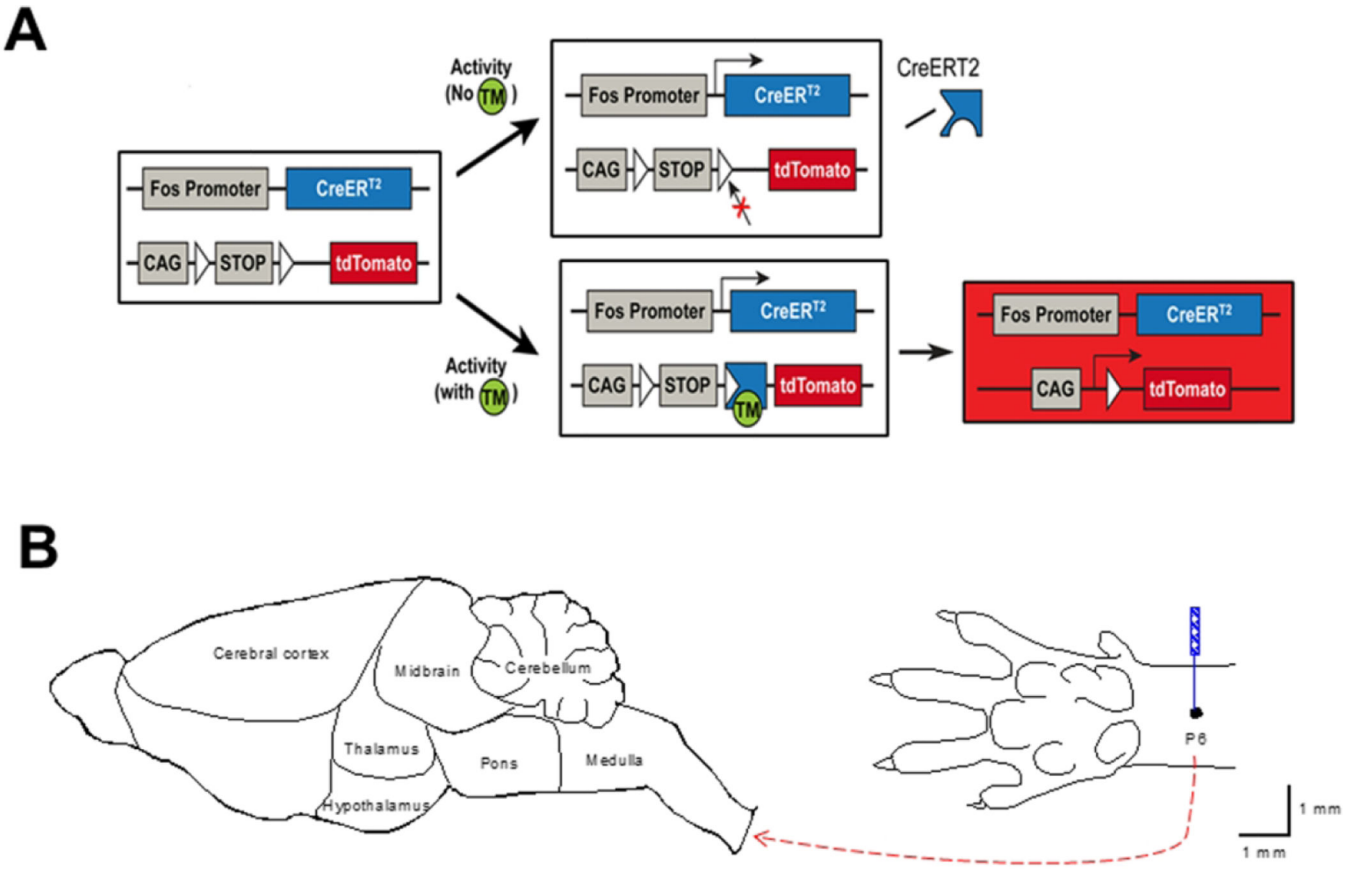

Figure 1.

The schematic of the approach used to identify neuronal activation throughout the forebrain following acupuncture. Panel A: illustration of the strategy of genetic capture of c-Fos active neurons using the Fos-CreER; Ai9 mouse (modified from Guenthner et al. 2013). The Fos-CreER mouse is crossed to a Cre reporter Ai9 mouse line to generate the Fos-CreER; Ai9 mouse to express tdTomato in Fos active neurons under the control of administration of the tamoxifen metabolite, 4-Hydroxytamoxifen (4-OHT). In the absence of 4-OHT, CreERT2 is retained in the cytoplasm of active cells, and no recombination can occur (top). The administration of 4-OHT causes CreERT2 to translocate to the nucleus so that active CreERT2-expressing cells can undergo Cre-mediated recombination and turn on permanent expression of the effector gene (e.g., tdTomato; bottom). Background recombination without administration of 4-OHT is very low in Fos-CreER; Ai9 mice. The activated neurons expressing c-Fos following stimulation are permanently labeled with tdTomato fluorescence protein that does not require immuno-enhancement for detection. Panel B: the diagram displays the outline of the mouse brain (*left*) and the site of the P6 acupoint located in the forelimb of the mouse (*right*).

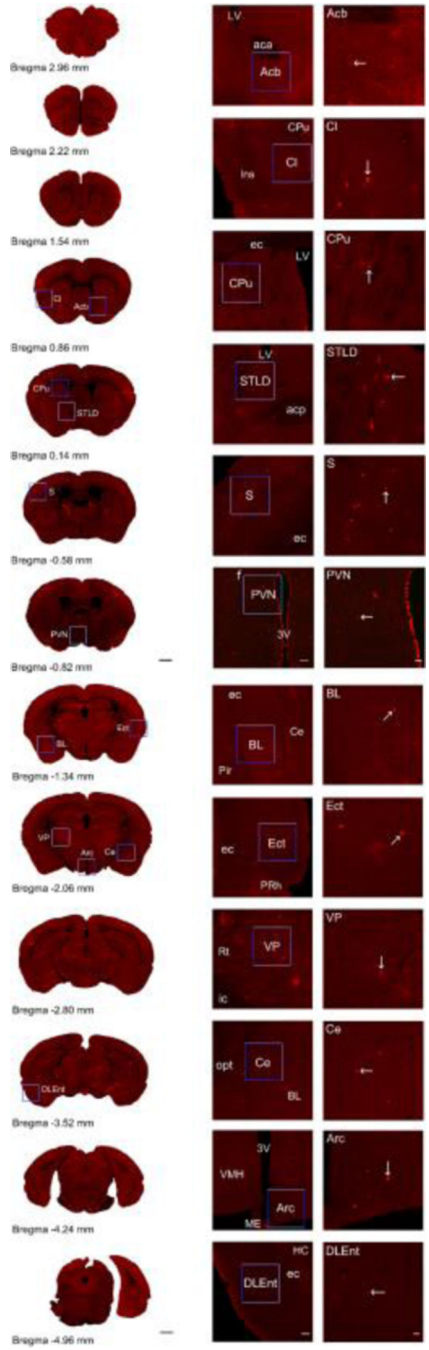

Figure 2.

Original tissue sections demonstrating c-Fos expression in higher brain regions of a representative mouse after P6 sham-acupuncture treatment. Prominent neuroanatomical locations are labeled in white for reference. Left column: images are showing selected brain sections; Middle and right columns: magnified regions those are shown within boxes in the left and middle columns, respectively. Labeled boxes correspond with labeled panels. Scale bars in panels on the bottom in the left, middle and right columns represent 1 mm, 100 μm, and 30 μm, respectively, which are applied to all panels in the same column. Arrows in the

right column indicate a neuron labeled with c-Fos. Bregma positions are consistent with Franklin & Paxino's mouse brain atlas (Franklin & Paxions. 2007). Abbreviations (white labels) in alphabetical order: 3V, third ventrical; aca, anterior commissure, anterior part; Acb, accumbens nucleus; acp, anterior commissure, posterior part; Arc, arcuate nucleus; BL, basolateral division of the amygdaloid nucleus; Ce, central division of the amygdaloid nucleus; Cl, claustrum; CPu, caudate putamen; DLEnt, dorsolateral entorhinal cortex; ec, external capsule; Ect, ectorhinal cortex; f, fornix; HC, Hippocampus; ic, internal capsule; Ins, insular cortex; LV, lateral ventricle; ME, median eminence; opt, optic tract; Pir, piriform cortex; PRh, perirhinal cortex; PVN, paraventricular nucleus; Rt, reticular nucleus (prethalamus); S, somatosensory cortex; STLD, dorsal part of the lateral division of the bed nucleus of the stria terminalis; VMH, ventromedial hypothalamic nucleus; VP, the ventral posterior division of the thalamic nucleus.

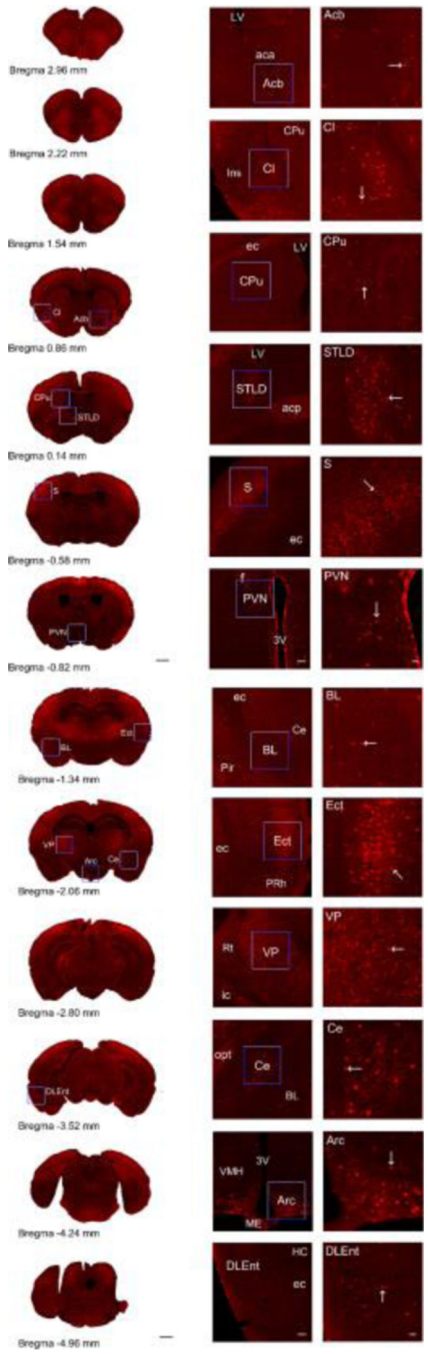

Figure 3.

Original tissue sections demonstrating c-Fos expression in the forebrain of one mouse treated with P6 acupuncture. Neuroanatomical locations labeled in white. Left column: images are showing selected brain sections; Middle and right columns: magnified regions those are shown within boxes in the left and middle columns, respectively. Labeled boxes correspond with labeled panels. Scale bars in panels on the bottom in the left, middle and right columns represent 1 mm, 100 μm, and 30 μm, respectively, which are applied to all panels in the same column. Arrows in the right column indicate a neuron labeled with c-Fos.

Bregma positions are consistent with Franklin & Paxino's mouse brain atlas (Franklin & Paxions. 2007). Abbreviations (white labels) in alphabetical order: 3V, third ventrical; aca, anterior commissure, anterior part; Acb, accumbens nucleus; acp, anterior commissure, posterior part; Arc, arcuate nucleus; BL, basolateral division of the amygdaloid nucleus; Ce, central division of the amygdaloid nucleus; Cl, claustrum; CPu, caudate putamen; DLEnt, dorsolateral entorhinal cortex; ec, external capsule; Ect, ectorhinal cortex; f, fornix; HC, Hippocampus; ic, internal capsule; Ins, insular cortex; LV, lateral ventricle; ME, median eminence; opt, optic tract; Pir, piriform cortex; PRh, perirhinal cortex; PVN, paraventricular nucleus; Rt, reticular nucleus (prethalamus); S, somatosensory cortex; STLD, dorsal part of the lateral division of the bed nucleus of the stria terminalis; VMH, ventromedial hypothalamic nucleus; VP, the ventral posterior division of the thalamic nucleus.

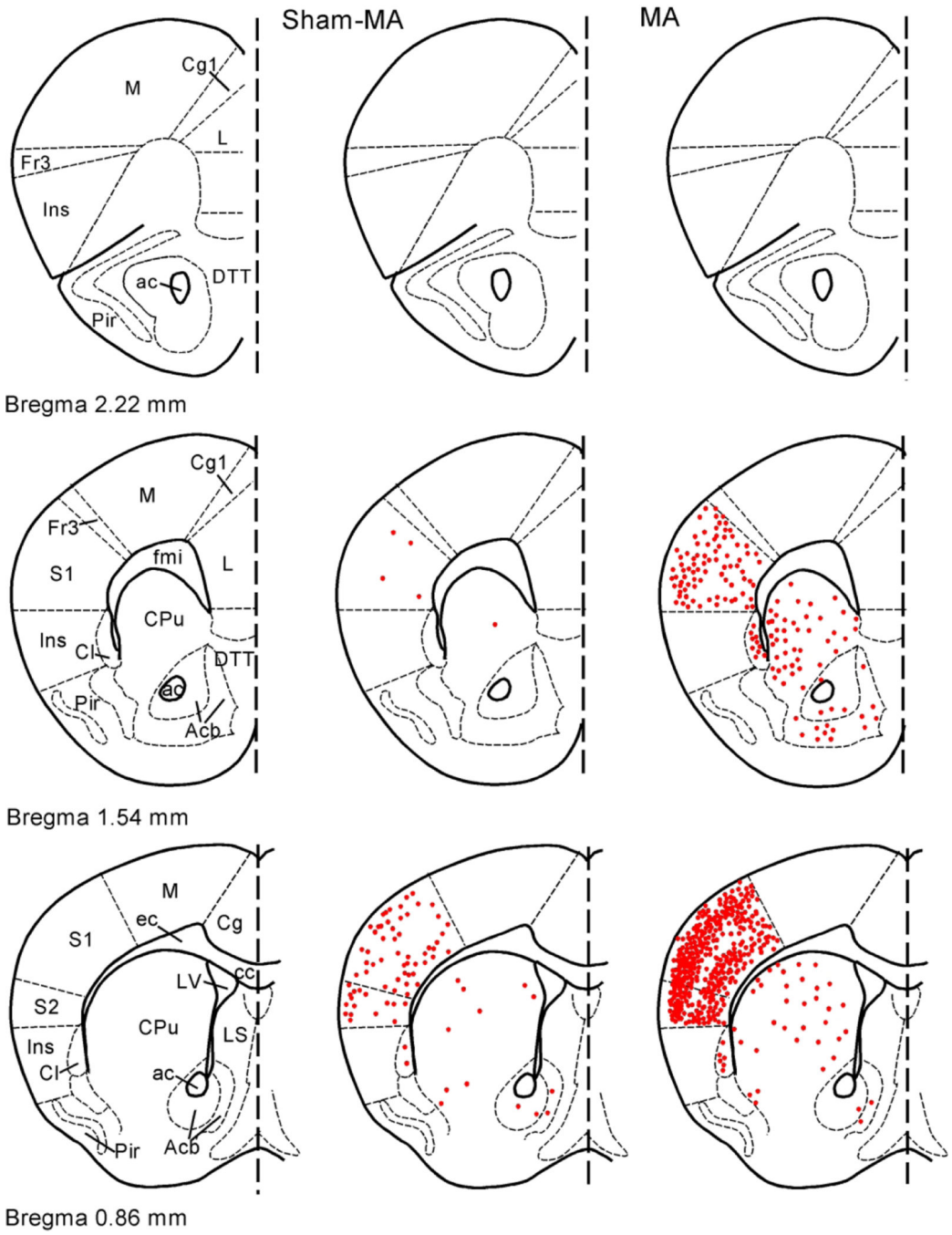

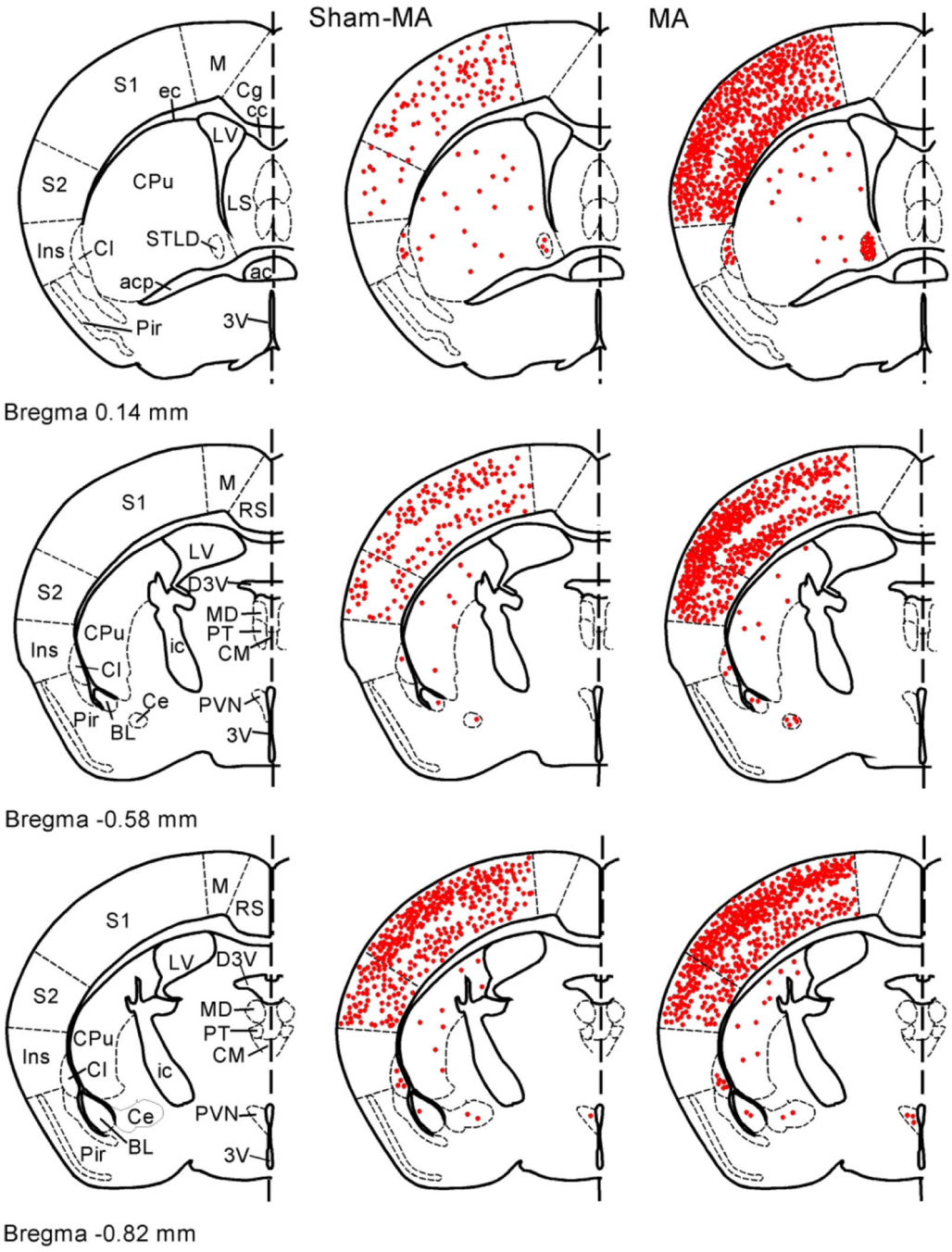

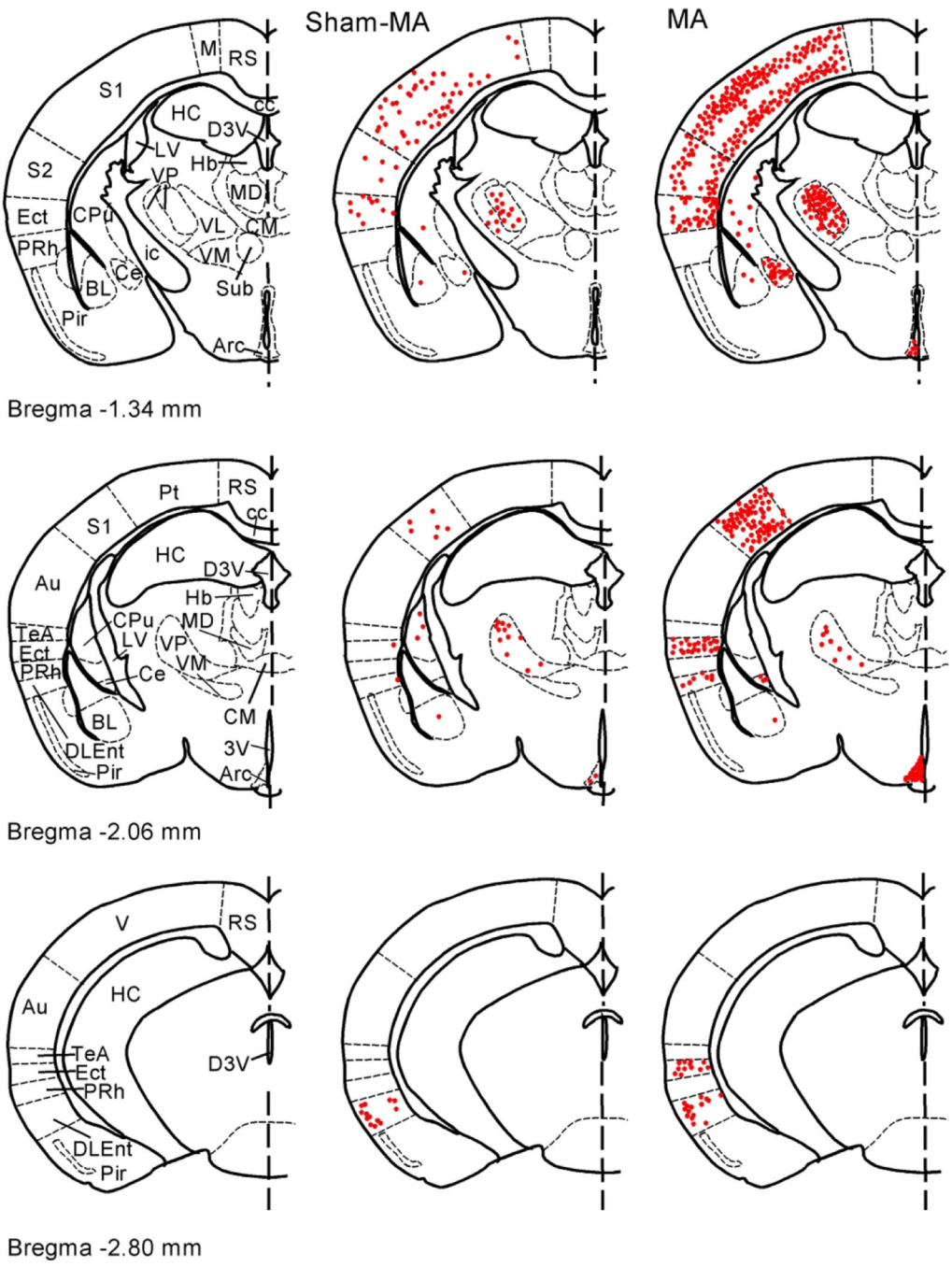

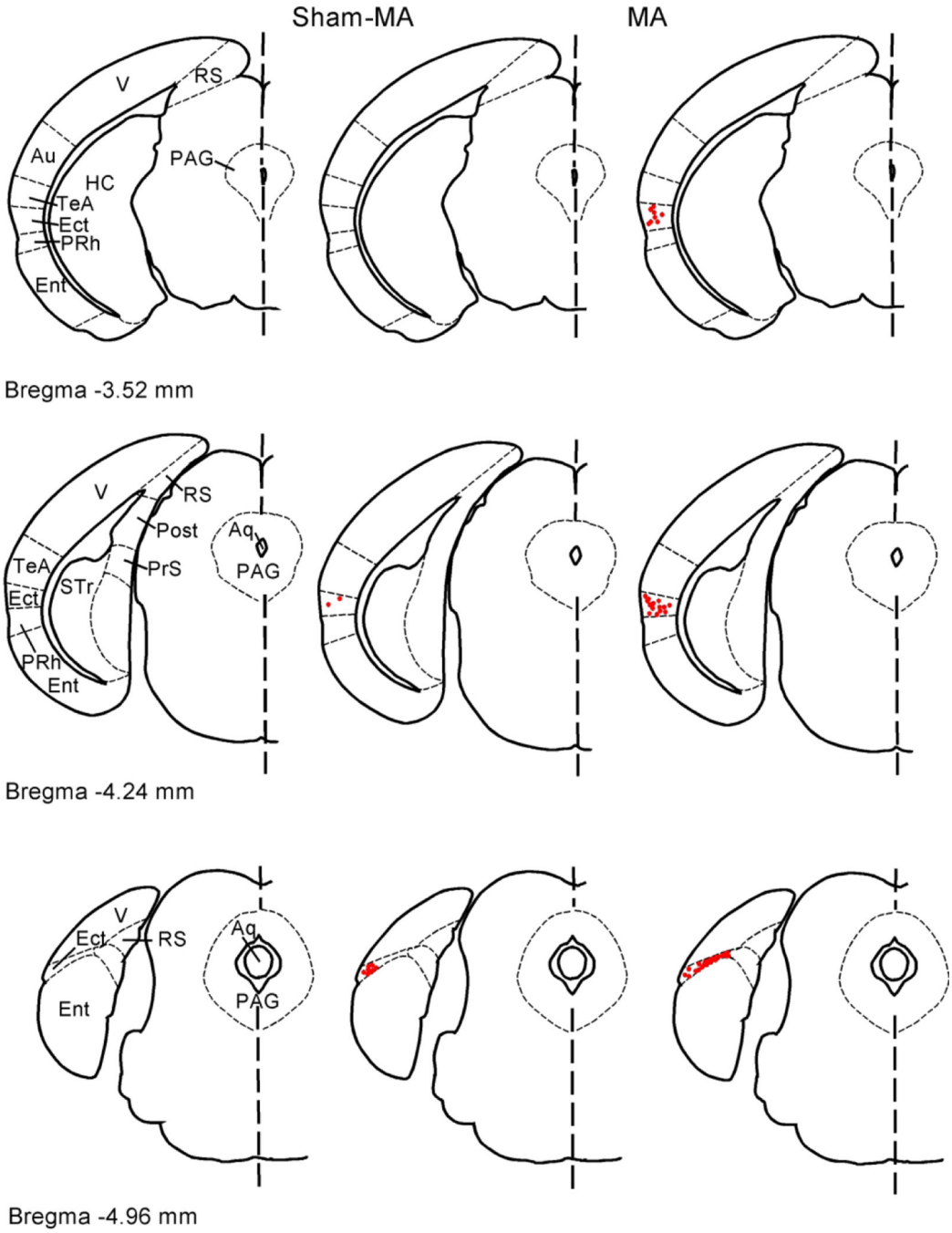

Figure 4.

Composite schematic maps showing overlay of c-Fos expression in specific regions of the forebrain following acupuncture or sham-acupuncture corresponding to atlas defined brain regions. The coronal sections of the forebrain are most closely matched to the stereotaxic planes displayed in Franklin & Paxino's mouse brain atlas (Franklin & Paxions. 2007) and correspond with the original brain sections demonstrated in Figures 2 and 3 of this study. Bregma positions between the ranges of 2.22 to −4.96 shown are consistent with mouse brain atlas. Each symbol (e.g., red dot) represents up to two c-Fos expressing cells. Areas in

which there is no significance in c-Fos expression between the two groups are not included for clarity. Abbreviations in alphabetical order: 3V, third ventricle; ac anterior commissure; Acb, core and shell of accumbens nucleus; aci, acp, posterior nerve of anterior commissure; Aq, aqueduct; Arc, arcuate nucleus; cc, corpus callosum; BL, basolateral amygdaloid nucleus; Ce, central amygdaloid nucleus; Cg1, area 1 of cingulate cortex; Cg, areas 1 and 2 of cingulate cortex; Cl, claustrum; CM, central medial thalamic nucleus; CPu, caudate putamen; DLEnt, dorsolateral entorhinal cortex; DTT, dorsal tenia tecta; ec, external capsule; DV3, dorsal third ventricle; Ect, ectorhinal cortex; fmi, forceps minor of the corpus callosum; Fr3, area 3 of frontal cortex; Hb, habenular nucleus; HC, hippocampus; ic, internal capsule; Ins, insular cortex; L, prelimbic and infralimbic cortex; LS, lateral septal nucleus; LV, lateral ventricle; M, primary and secondary motor cortices; MD, mediodorsal thalamic nucleus; PAG, periaqueductal gray; PRh, perirhinal cortex; PrS, presubiculum; Pir, piriform cortex; Post, postsubiculum; Pt, paratenial cortex; PT, paratenial thalamic nucleus; PVN, paraventricular hypothalamic nucleus; RS, retrosplenial cortex; S1, primary somatosensory cortices; S2, secondary somatosensory cortices; STLD, dorsal part of the lateral division of the BNST; STr, transition area of the subiculum; Sub, submedius thalamic nucleus; TeA, temporal association cortex; VL, ventrolateral thalamic nucleus; VM, ventromedial thalamic nucleus; VP, posterior parts of the ventral thalamic nucleus.

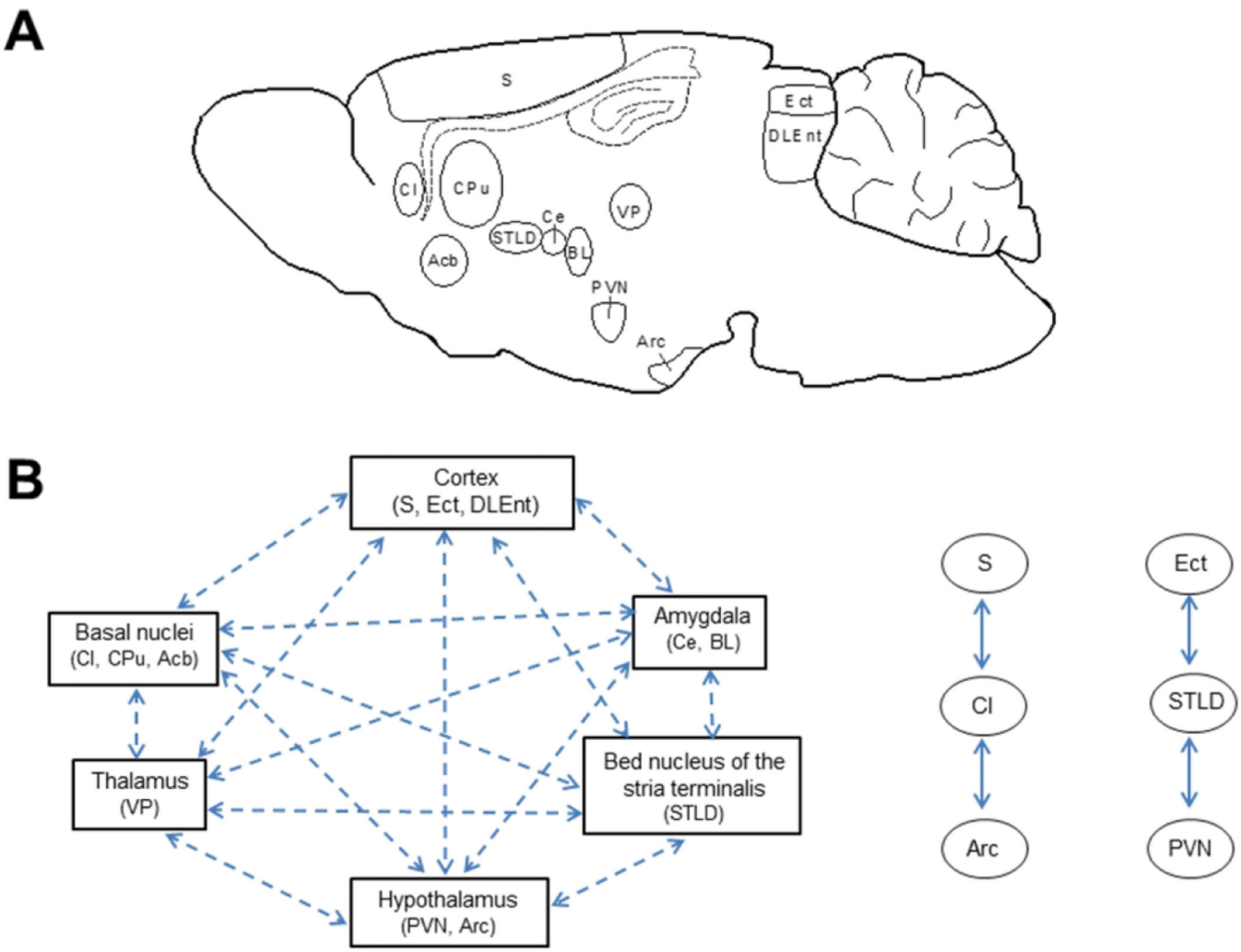

Figure 5.

Patterns of potential network activation by manual acupuncture (MA). Panel A: the schematic indicates c-Fos expression in the nuclei throughout the forebrain following MA at P6, which is significantly increased in comparison with sham-MA controls (see Fig. 4 and Table 1). Panel B: Dash lines (*left side*) indicate possible correlations of forebrain nuclei activated by MA at P6 (see Table 2). Solid lines (*right side*) indicate significant relationships between two nuclei, as determined by Pearson correlation analysis. Abbreviations in alphabetical order: Acb, accumbens nucleus; Arc, arcuate nucleus; BL, basolateral division of the amygdaloid nucleus; Ce, central division of the amygdaloid nucleus; Cl, claustrum; CPu, caudate putamen; DLEnt, dorsolateral entorhinal cortex; Ect, ectorhinal cortex; PVN, paraventricular nucleus; S, somatosensory cortex; STLD, dorsal part of the lateral division of the bed nucleus of the stria terminalis; VP, the ventral posterior division of the thalamic nucleus.

Table 1.

Fos expression in the forebrain regions following manual acupuncture at the P6 acupoint

		Treatment		
		Sham-acupuncture (n=5)	Acupuncture (n=5)	P value
Cortex				
FrA	Frontal association cortex	18 ± 11	209 ± 77	0.057
Fr3	Frontal cortex, area 3	17 ± 6	44 ± 12	0.082
M	Primary & Secondary motor cortex	124 ± 43	166 ± 36	0.470
S	Primary & Secondary somatosensory cortex	204 ±105	1225 ± 315	0.009*
	S1 Primary somatosensory cortex	169 ± 90	934 ± 232	0.010*
	S2: Secondary somatosensory cortex	35 ± 15	291 ± 95	0.036*
Cg1	Cingulate cortex, area 1	15 ± 6	33 ± 8	0.103
Cg	Cingulate cortex, areas 1 & 2	27 ± 13	84 ± 31	0.121
L	Prelimbic (PrL) and Infralimbic (IL) cortex	27 ± 23	64 ± 13	0.400
DTT	Dorsal tenia tecta	19 ± 5	16 ± 5	0.677
Pir	Piriform cortex	42 ± 23	73 ± 18	0.322
Ins	Insular cortex, granular, dys/agranular	23 ± 7	67 ± 22	0.086
RS	Retrosplenial cortex	71 ± 22	158 ± 29	0.045
Ect	Ectorhinal cortex	15 ± 6	60 ± 14	0.016*
PRh	Perirhinal cortex	7 ± 2	23 ± 6	0.044
DLEnt	Dorsolateral entorhinal cortex	3 ± 1	11 ± 3	0.024*
Pt	Parietal cortex, medial & lateral, posterior	142 ± 80	396 ± 65	0.042
TeA	Temporal association cortex	13 ± 5	21 ± 4	0.301
PrS	Presubiculum	5 ± 2	41 ± 10	0.009
Post	Postsubiculum	39 ± 17	164 ± 32	0.008
Str	Subiculum, transition area	16 ± 7	31 ± 4	0.112
V	Visual cortex	345 ±196	686 ±139	0.195
Septal nucleus				
LS	Lateral septal nucleus	8 ± 3	11 ± 1	0.306
Basal nuclei				
CPu	Caudate putamen	14 ± 4	30 ± 4	0.020*
Acb	Accumbens nucleus	5 ± 2	18 ± 3	0.006*
CI	Claustrum	6 ± 2	18 ± 4	0.036*
Amygdala				
Ce	Central division of amygdaloid nucleus	1 ± 1	24 ± 12	0.008*
BL	Basolateral division of amygdaloid nucleus	2 ± 1	5 ± 2	0.041*
Bed nucleus of the stria terminalis				
STLD	Lateral division, dorsal part of bed nucleus	5 ± 2	40 ± 6	0.020*
Thalamus				
VP	Ventral posterior division of thalamic nucleus	19 ± 6	59 ± 12	0.018*

		Treatment		
		Sham-acupuncture (n=5)	**Acupuncture (n=5)**	**P value**
	Lateral portion of VP (VPL)	5 ± 1	17 ± 5	0.049*
	Medial portion of VP (VPM)	14 ± 5	42 ± 10	0.056
VL	Ventrolateral division of thalamic nucleus	29 ± 12	31 ± 4	0.871
VM	Ventromedial division of thalamic nucleus	13 ± 8	9 ± 3	0.690
MD	Mediodorsal division of thalamic nucleus	6 ± 3	15 ± 4	0.102
CM	Central medial division of thalamic nucleus	9 ± 5	17 ± 6	0.310
Sub	Submedius division of thalamic nucleus	14 ± 8	11 ± 2	0.667
Hb	Habenular nucleus	3 ± 1	5 ± 2	0.548
PT	Paratenial thalamic nucleus	5 ± 3	21 ± 8	0.074
Hypothalamus				
PVN	Paraventricular nucleus	0 ± 0	13 ± 5	0.029*
Arc	Arcuate hypothalamic nucleus	9 ± 4	23 ± 3	0.023*
Midbrain				
PAG	Periaqueductal gray	4 ± 1	6 ± 2	0.290

Means ± SE. Average number (#) of c-Fos positive cells per section in the forebrain of the Fos-CreER mouse. P value, acupuncture-treated group vs. control group.

* indicates $P < 0.05$.

Table 2.

Pearson correlation for Fos expression in the forebrain regions following manual acupuncture at the P6 acupoint

Correlation with PVN										
S	CI	Ect	DLEn	CPu	Acb	Ce	BL	STLD	VP	Arc
r=0.767	r=0.620	r=0.759	r=0.382	r=0.244	r=0.121	r=0.201	r=0.654	**r=0.921** *	r=0.768	r=−0.292
p=0.130	p=0.264	p=0.137	p=0.525	p=0.693	p=0.847	p=0.847	p=0.231	**p=0.023**	p=0.130	p=0.633
Correlation with S										
	CI	Ect	DLEn	CPu	Acb	Ce	BL	STLD	VP	Arc
	r=0.926 *	r=0.297	r=−0.157	r=−0.425	r=0.216	r=−0.172	r=0.703	r=0.590	r=0.770	r=−0.661
	p=0.024	p=0.627	p=0.801	p=0.475	p=0.839	p=0.782	p=0.185	p=0.295	p=0.128	p=0.224
Correlation with CI										
		Ect	DLEn	CPu	Acb	Ce	BL	STLD	VP	Arc
		r=0.274	r=−0.078	r=−0.556	r=−0.041	r=−0.382	r=0.798	r=0.439	r=0.476	**r=−0.893** *
		p=0.655	p=0.901	p=0.331	p=0.947	p=0.526	p=0.106	p=0.459	p=0.418	**p=0.041**
Correlation with Ect										
			DLEn	CPu	Acb	Ce	BL	STLD	VP	Arc
			r=0.659	r=0.621	r=−0.685	r=−0.008	r=0.684	**r=0.896** *	r=0.235	r=−0.166
			p=0.226	p=0.263	p=0.202	p=0.989	p=0.203	**p=0.039**	p=0.703	p=0.790
Correlation with DLEnt										
				CPu	Acb	Ce	BL	STLD	VP	Arc
				r=0.666	r=−0.351	r=0.450	r=0.122	r=0.381	r=−0.158	r=0.252
				p=0.220	p=0.562	p=0.447	p=0.846	p=0.521	p=0.491	p=0.682
Correlation with CPu										
					Acb	Ce	BL	STLD	VP	Arc
					r=−0.391	r=0.482	r=−0.127	r=−0.405	r=0.412	r=0.767
					p=0.515	p=0.411	p=0.839	p=0.499	p=0.130	p=0.130
Correlation with Acb										
						Ce	BL	STLD	VP	Arc
						r=0.573	r=−0.609	r=−0.405	r=0.412	r=0.252
						p=0.312	p=0.275	p=0.499	p=0.491	p=0.682
Correlation with Ce										
							BL	STLD	VP	Arc
							r=−0.585	r=0.055	r=0.327	r=0.629
							p=0.300	p=0.930	p=0.592	p=0.256
Correlation with BL										
								STLD	VP	Arc
								r=0.699	r=0.264	r=−0.770
								p=0.189	p=0.668	p=0.128
Correlation with STLD										
									VP	Arc
									r=0.629	r=−0.162

	p=0.255	p=0.795
Correlation with VP		
		Arc
		r=0.031
		p=0.961

Pearson correlation values (r) and corresponding p-values were assessed to identify the correlation of each of brain regions of rats treated with manual acupuncture, in those brain area the number of Fos-immunoreactive cell was significantly increased in comparison with controls (see Table 1).

* indicates significant correlation ($p < 0.05$). Abbreviations: PVN, paraventricular nucleus; S, primary and secondary somatosensory cortex; CI, claustrum; Ect, ectorhinal cortex; DLEnt, dorsolateral entorhinal cortex; CPu, caudate putamen; Acb, accumbens nucleus; Ce, central division of amygdaloid nucleus; BL, basolateral division, anterior part of amygdaloid nucleus; STLD, lateral division, dorsal part of bed nucleus; VP, ventral posterior division of thalamic nucleus; Arc, arcuate hypothalamic nucleus.